Antenna Tracking Techniques for Long Range Air-to-Ground Communication Systems Using a Monopulse Method

JAESIN KIM[1,2], JAEMOON LEE[2], AND INKYU LEE [1], (Fellow, IEEE)

[1]School of Electrical Engineering, Korea University, Seoul 02841, South Korea
[2]The 2nd Research and Development Institute, Agency for Defense Development, Daejeon 34186, South Korea

Corresponding author: Inkyu Lee (inkyu@korea.ac.kr)

ABSTRACT In this paper, we consider long range air-to-ground (AG) communication systems which support airborne platforms including unmanned aerial vehicles (UAVs) for real-time applications. In this system, we design tracking techniques for directional ground antennas which enable reliable AG communication regardless of dynamic maneuvers of the UAV. We apply a simple monopulse method and a fixed gain filtering algorithm to develop a single channel monopulse tracking system with an angular estimation filtering, which exploits a downlink signal without requiring a dedicated channel. Through the AG communication prototype and realistic flight tests, we evaluate the tracking accuracy performance at the distance of hundreds of kilometers and demonstrate the auto-tracking capability of the angular estimation filter. The flight test results show that the tracking accuracy of our proposed system is sufficient for long range transmission with a narrow beam antenna. Also, in the absence of the downlink signal, it is observed that the ground prototype can resume the monopulse tracking procedure, and successfully maintains the tracking accuracy.

INDEX TERMS Air-to-ground communication systems, antenna tracking, estimation filter, monopulse.

I. INTRODUCTION

In recent years, there have been increasing interests in utilizing airborne platforms for various real-time applications such as military reconnaissance, disaster monitoring, border patrol, and airborne communication networks [1], [2]. Especially, unmanned aerial vehicles (UAVs) have received more attentions as a useful aerial platform [3]–[5]. Now, various UAV enabled networks have been introduced [6]–[11]. For such an aerial system, a seamless air-to-ground (AG) communication is essential which establishes a common wireless link between an air data terminal (ADT) of the airborne platform and a ground data terminal (GDT) of the ground control station.

Depending on the purpose of its application and data characteristic, the AG communication link can be classified into a cellular network centric link and a mission related link. The first one indicates the AG wideband backhaul that connects wired backbone networks on the ground to aerial

The associate editor coordinating the review of this manuscript and approving it for publication was Xingwang Li [ID].

base stations, e.g., UAV assisted cellular networks [12], while the second one represents a link which sends secured data and streaming video data collected by sensors of the airborne platform to the ground control station [13], [14].

Both types of links have to transmit a massive amount of gathered data through the AG wireless channel, rather than through a satellite system with limited capacity. However, it is not straightforward to apply conventional terrestrial techniques into the AG communication system, since high maneuverability of aerial nodes has not been properly considered. Moreover, if the AG communication system uses high frequency bands such as X or Ku bands which usually suffer from a large free-space path loss, it is difficult to operate in a wide area. Therefore, the AG communication system practically needs high-gain directional antennas which can cover hundreds of kilometers. Thus, accurate pointing and tracking are required to ensure a maximum gain during dynamic airborne maneuvers. Some works studied the AG communication system in the context of directional tracking antennas [15]–[19]. However, they are still limited in UAV systems with short coverage and low altitude.

Originally, a tracking radar can measure a direction of arrival (DOA) of a signal that radiates from a distant target or a reflected signal. To this end, a tracking antenna of radar systems tries to keep the antenna beam axis aligned with a mobile target. The related technologies can be typically classified into sequential and simultaneous lobing methods [20]. The sequential lobing is divided into lobe switching and conical scan methods. On the other hand, the simultaneous lobing, also known as monopulse, includes amplitude and phase comparison monopulse techniques.

In the monopulse, two-coordinate systems normally require three receiver channels, i.e., sum, azimuth difference, and elevation difference channels. Each channel has its respective intermediate frequency (IF) channel. In fact, the performance gains of the monopulse over sequential lobing schemes are obtained at the expense of increased complexity and cost. Although two or single channel systems conventionally impose some losses in performance, we practically obtain simple monopulse systems that might be adequate for special applications. Hence, in terms of reducing the number of the receiver channels, many literatures have proposed simple monopulse systems [20], [21].

In this paper, we develop a single channel monopulse tracking system with additional estimation filtering for the wideband and long range AG communication systems. Motivated by the channel reducing methods reported in [20] and [22], we focus on a simplified single channel approach that requires only one IF chain for the monopulse method. The proposed single channel monopulse tracking is based on an amplitude comparison. Especially, by subtracting the out-of-phase signal and adjusting two parameters, we demonstrate that the proposed single channel monopulse technique with reduced complexity obtains the performance almost identical to the conventional three channel system.

In addition, we adopt the monopulse tracking architecture exploiting a downlink signal without requiring additional dedicated channels. Besides, for the case where the downlink signal is not available, we employ an angular estimation procedure with low complexity. Utilizing a simple form of the estimation filter in [23], we combine the monopulse tracking system and the tracking angle based estimation filter. Moreover, we implement the AG communication system prototype and present extensive experimental results acquired from actual flight tests at the distance of hundreds of kilometers. In our test, the flight maneuvers include straight-and-level flights as well as turns, climbs, and descending flights.

To the best of our knowledge, no literature has investigated the monopulse tracking system for the long rage AG communication system yet. Authors in [15] proposed a steering algorithm to provide backhaul connectivity between a UAV and a ground base station, and tested a simple experimental setup. The work [22] analyzed angle estimation methods for orthogonal frequency division multiplexing based single channel monopulse tracking in the UAV AG communications. Also, the aerial communication techniques were developed in [17]–[19] with the alignment of directional antennas to
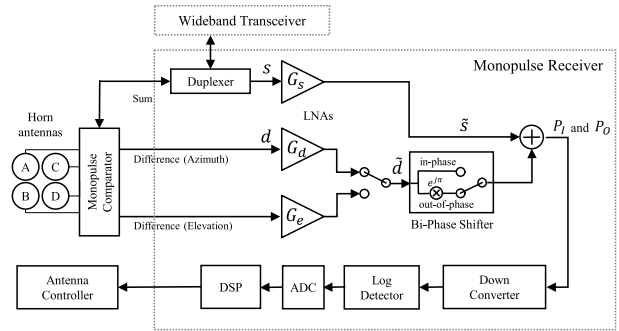

FIGURE 1. Block diagram of the single channel monopulse tracking system in the GDT.

enable long distance and broadband air-to-air systems. However, the field test was conducted only at the distance of hundreds of meters [18]. Therefore, our paper presents a practically significant study for long range commercial and military applications in large airborne platforms.

The remainder of this paper is organized as follows: In Section II, we investigate the proposed single channel monopulse system. Section III applies a modified angular filter with our proposed single channel monopulse tracking. Under various flight conditions, the test setup and results are presented in Section IV, and conclusions are followed in Section V.

II. SIMPLIFIED SINGLE CHANNEL MONOPULSE TRACKING SYSTEM

In this paper, we apply a single channel monopulse technique to the GDT of the AG communication system for wideband and long range communications. Here, it is crucial to strike a balance between a precise tracking capability and a long range requirement. In the following, we briefly explain the ground system diagram for the AG communication system in Fig. 1 and describe the procedure for generating the monopulse output known as the error signal.

As shown in Fig. 1, the monopulse tracking system in the GDT consists of four horn antennas, a monopulse comparator, low noise amplifiers (LNAs), a bi-phase shifter, a digital signal processor (DSP) block, and analog-to-digital converter (ADC). We can see that the monopulse receiver has a single IF channel. The proposed single channel monopulse tracking system is categorized as an amplitude comparison system.

The four quadrants A, B, C, and D of Fig. 1 represent the corresponding signals of four feed horns. At the front-end of the monopulse receiver, the monopulse comparator forms the sum s, the azimuth difference d, and the elevation difference[1] output signals by means of hybrid junctions[1]. More detailed operations of a monopulse comparator is described

---

[1] For simplicity, we only describe the sum signal and the difference signal of an azimuth coordinate in this paper. The same procedure can be applied to the elevation coordinate. Unless stated otherwise, the difference signal means an azimuth difference signal.

in [20] and [24]. The sum and difference signals are obtained as $s = A+B+C+D$ and $d = (A+B)-(C+D)$, respectively, which depend on individual horn antenna's patterns, squint angles and monopulse comparators.

Next, the monopulse receiver produces the monopulse output by using imbalance of power derived from the sum and difference signals. With the resultant monopulse output, the antenna controller drives a servo motor subsystem for mechanically rotating the GDT antenna. After amplifying the monopulse comparator output in the LNAs, the azimuth difference signal and the elevation difference signal are multiplexed in time division mode in the switch as illustrated in Fig. 1. Denoting the dB-scale gain of the LNAs in the sum and azimuth difference signal path as G_s and G_d, respectively, the amplified signals in each path are indicated as $\tilde{s} = 10^{G_s/20}s$ and $\tilde{d} = 10^{G_d/20}d$. With the multiplexed azimuth difference signal, the bi-phase shifter generates the in-phase and out-of-phase signals about the difference signal.

Then, the signal combiner couples these two outputs with the sum signal individually. Processing $s + d$ and $s - d$ instead of s and d is advantageous in two-coordinate tracking systems [20]. Since our system ignores a relative phase between the sum and difference signals, it is insensitive to phase imbalance in the receiver channel. By considering an equal power combiner, the combined in-phase power P_I and the out-of-phase power P_O can be computed as $P_I = \frac{1}{2}(\tilde{s} + \tilde{d})^2$ and $P_O = \frac{1}{2}(\tilde{s} - \tilde{d})^2$. Finally, these are converted to IF signals by mixing with a frequency of a local oscillator, and then detected at a logarithmic power detector. A log operation in the power detector makes the monopulse output proportional to the angle off axis [20].

Let us introduce η as the proposed monopulse output. Interestingly, we can obtain the monopulse output η from the difference between P_I and P_O. By subtracting P_O from P_I in terms of dBm unit and denoting M as the scaling factor designed at the DSP block, the monopulse output is derived as

$$\eta \triangleq M\left(10\log P_I - 10\log P_O\right) \tag{1}$$

$$= M\left(20\log\left(\tilde{s}+\tilde{d}\right) - 20\log\left(\tilde{s}-\tilde{d}\right)\right) \tag{2}$$

$$= 20M\log\frac{1+\tilde{d}/\tilde{s}}{1-\tilde{d}/\tilde{s}}. \tag{3}$$

At last, by expressing the gap of the amplifier gain between the sum and difference paths as $K = 10^{(G_d-G_s)/20}$, the monopulse output is written as

$$\eta = 20M\log\frac{1+K\,(d/s)}{1-K\,(d/s)}. \tag{4}$$

Now, based on the numerical method established in [25], we can obtain the desired values on K and M within the angles of interest. In Fig. 2, we can see that our monopulse output becomes almost identical to the baseline three channel's output by fixing $K = 0.11$ and $M = 0.5$. Here, the baseline three channel monopulse output $\bar{\eta}$ is defined as $\bar{\eta} \triangleq d/s$ [20]. Typically, the monopulse system is designed
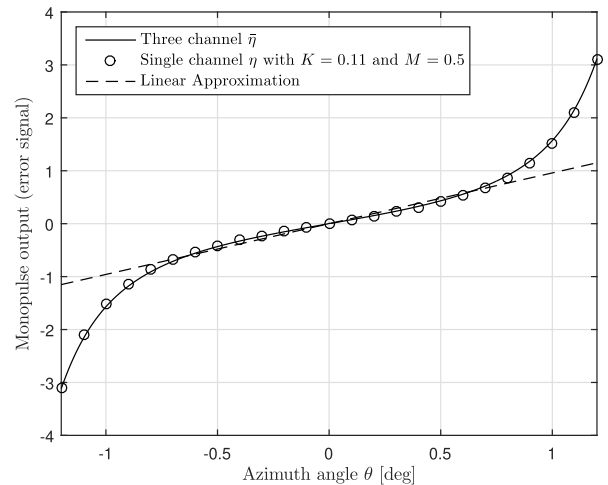

FIGURE 2. Comparison among monopulse outputs.

such that the monopulse output is linear within the half-power beam width (HPBW) of the sum pattern [26]. Thanks to the linearity, we can take a simple one-shot solution to extract a tracking angle. The figure shows that the linear approximation matches well between $-0.7°$ and $0.7°$, where the prototype antenna pattern with the HPBW of $1.4°$ will be explained in Section IV.

The proposed tracking system utilizes phase shift keying (PSK) modulated signals transmitted from the ADT's wideband transceiver. The conventional monopulse tracking system normally requires dedicated pulse signals via separate channels to estimate the direction of a target [20], [27]. From Fig. 1, we can find that the duplexer connects the downlink signal to both the wideband transceiver and the monopulse receiver. Obviously, since the duplexer offers a two-way operation for both uplink and downlink, the same sum pattern is shared on transmission and reception of the wideband transceiver. As a result, this architecture combined with the single channel approach allows to make the GDT system simple, because it is not necessary to allocate additional frequency resources such as a beacon channel.

III. ANGULAR ESTIMATION FILTERING FOR AUTO-TRACKING

In this section, we address an angular estimation procedure for the antenna controller in Fig. 1 to obtain an auto-tracking capability. As explained in the previous section, we adopt the monopulse tracking architecture exploiting a downlink signal. During the flight, poor radio propagation circumstances can happen due to airframe shadowing and blocking from terrain obstructions. Specifically, to cope with the absence of the downlink signal, the GDT needs to be able to automatically trace the ADT for a certain period of time without any monopulse output.

To tackle our problem of interest, we here consider a critically damped filter, which is a special type of fixed gain filtering algorithms such as the α-β filter [23], [28]. The filter usually provides good performance with low computational cost
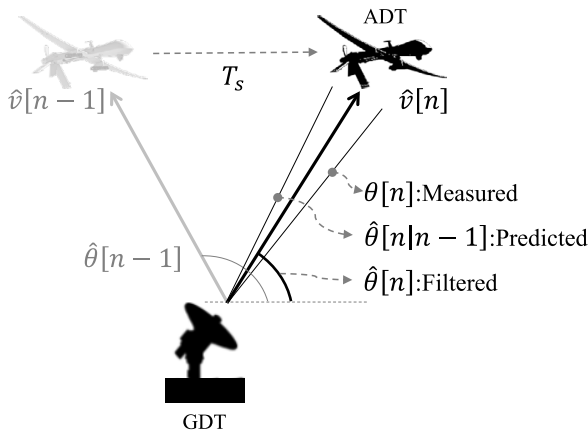
FIGURE 3. Angular estimation filtering.

in many fields. Although it is well-known that the Kalman filter is optimal in terms of minimizing the variance of the estimation error, it requires the characteristics of the model behavior including the process noise and the measurement noise [29]. In practice, it may be difficult to identify such priori information [30].

To solve this issue, we develop a simple angular estimation filter based on the azimuth angle[2] and angular velocity information as illustrated in Fig. 3. We assume that the aircraft travels with a constant angular velocity. This assumption is reasonable if the time between observations or the angular acceleration of the aircraft is small [28]. In particular, we adjust our filter gains by utilizing relative angle variations to take into account unexpected maneuvers.

Let us denote $\hat{\mathbf{x}}[n|n-1] \triangleq [\hat{\theta}[n|n-1] \ \hat{v}[n|n-1]]^T$ where $\hat{\theta}[n|n-1]$ and $\hat{v}[n|n-1]$ indicate the prediction estimates about the azimuth angle and the angular velocity, respectively, as the prediction estimate at time n based on the past measurements. From Fig. 3, we have the following transition equation as

$$\hat{\mathbf{x}}[n|n-1] = \mathbf{F}\hat{\mathbf{x}}[n-1|n-1] \tag{5}$$

where the transition matrix $\mathbf{F}$ is given as $\mathbf{F} = \begin{bmatrix} 1 & T_s \\ 0 & 1 \end{bmatrix}$ with T_s being the time between estimates, and $\hat{\mathbf{x}}[n-1|n-1]$ is the filtered estimate at time $n-1$.

Next, we can obtain the filtered estimate $\hat{\mathbf{x}}[n|n] \triangleq [\hat{\theta}[n] \ \hat{v}[n]]^T$ at time n based on the present measurement as well as the past measurements as

$$\hat{\mathbf{x}}[n|n] = \hat{\mathbf{x}}[n|n-1] + \mathbf{W}_n(\theta[n] - \mathbf{H}\hat{\mathbf{x}}[n|n-1]) \tag{6}$$

where $\mathbf{W}_n$ denotes a filter gain vector of length 2, $\theta[n]$ represents the azimuth angle measurement in the monopulse receiver at time n, and the measurement vector $\mathbf{H}$ is defined as $\mathbf{H} = [1 \ 0]$. If there is no measurement on $\theta[n]$ due to the

[2] The same procedure can be applied to the elevation coordinate. When tracking in azimuth and elevation angle, one might run multiple filters in parallel. However, we adopt the filtering in azimuth coordinate only because the angle variation over the elevation axis is relatively limited in most flights.

absence of the downlink signal, the last estimate is used, i.e. $\theta[n]$ is set to $\hat{\theta}[n|n-1]$.

In the critically damped filter [23], $\mathbf{W}_n$ has constant gain coefficients. However, the angular velocity normally varies with a trajectory, and there exist deviations from a cruise flight practically. Therefore, to consider the irregular change of the angular velocity, $\mathbf{W}_n$ is rewritten as

$$\mathbf{W}_n = \begin{bmatrix} 1 - (\xi_{init} - \xi_N[n])^2 \\ \dfrac{1}{T_s}(1 - (\xi_{init} - \xi_N[n]))^2 \end{bmatrix} \tag{7}$$

where ξ_{init} denotes an initial smoothing value, and $\xi_N[n] \triangleq \epsilon \left| \dfrac{1}{N} \sum_{l=0}^{N-1} ((\hat{\theta}[n-l] - \hat{\theta}[n-1-l])/\hat{\theta}[n-l]) \right|$ represents a moving average with respect to the ratio of the angle change over a period of N. Here, ϵ is an arbitrary constant for $0 \leq \epsilon \leq 1$. Note that this approach using the ratio of change between consecutive data is suitable for taking into account a maneuvering trend [31], [32]. For $0 \leq \xi_{init} \leq 1$ and $0 \leq \xi_N[n] \leq 1$, when $\xi_{init} - \xi_N[n]$ term gets closer to 1, we have a heavy smoothing effect. As $\xi_N[n]$ increases, the filter gain coefficients become more associated with the present measurement. Consequently, by averaging the ratio of angle changes at every time in a sliding window fashion, $\mathbf{W}_n$ has adoptive gain coefficients over time.

IV. FLIGHT TEST RESULTS

In this section, we present field test results for the single channel monopulse tracking technique combined with the angular estimation filter. For simulations, we implement the experimental AG communication system employing the proposed scheme and conduct flight tests under realistic scenarios. Throughout the flight test, we focus on evaluating the tracking accuracy at long distances and the auto-tracking capability during temporary disconnections.

A. EXPERIMENTAL SETUP

In the GDT antenna part, we employ an axially displaced elliptical (ADE) dual reflector antenna with a diameter of 60λ, where λ is a wavelength. The ADE type provides high efficiency with compact mechanical designs [33]. We offer the measured sum s and difference d gain patterns and the GDT prototype in Fig. 4. In particular, the shape of the sum pattern shows a pencil beam with the HPBW of $1.4°$. This directional pattern is indispensable for long range communications. At the boresight angle, the null depth of the difference pattern is given as more than 40 dB, which is important for the tracking performance [33].

The proposed scheme can be applied to both unmanned and manned aircraft systems. For a safe and effective flight test, the manned aircraft Cessna 208 Caravan is used in our experiment. Regarding the ADT prototype, the aircraft configuration is similar to the ground site, where most components are installed inside the aircraft. The transceiver provides a wideband X band connectivity at experimental target regions by supporting a high power amplifier with a bandwidth of up
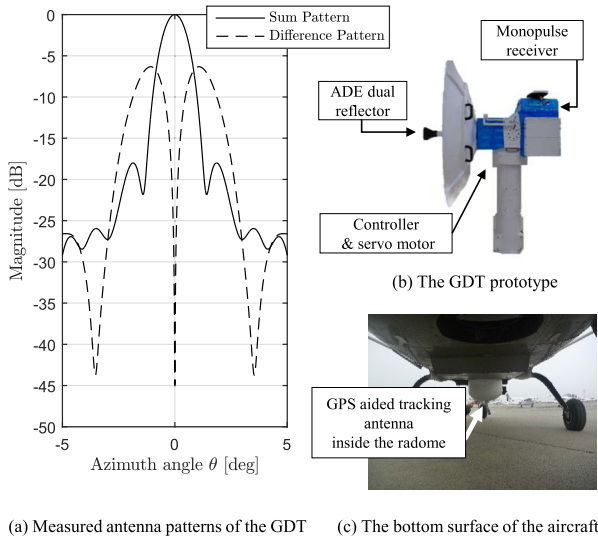
(a) Measured antenna patterns of the GDT   (c) The bottom surface of the aircraft

(b) The GDT prototype

FIGURE 4. The measured GDT antenna patterns and the implemented prototypes.

FIGURE 5. Tracking accuracy result in the region R1.

FIGURE 6. Tracking accuracy result in the region R3.

to tens of MHz. Specifically, a dual-axis, global positioning system (GPS) aided[3] X-band tracking antenna with an aperture coupled patch array is mounted on the bottom surface of the aircraft as shown in Fig. 4. The flight speed is set to 270 to 300 km/h during all flights. The flight trajectories have been pre-defined such that clear radio line-of-sight (LOS) can be maintained in term of the antenna's field of view.

During whole tests, the GDT prototype uses the monopulse output curve generated with $K = 0.11$, and $M = 0.5$ in Eq. (4) of Section II. The angular estimation filtering parameters in Section III are set as $\xi_{init} = 0.99$ and $\epsilon = 0.9$ which are determined from extensive computer simulations. This means that $\hat{\theta}[n|n-1]$ predicted with past measurements is more reliable than current measurement $\theta[n]$. Also, we fix $N = 200$ and $T_s = 10$ ms such that T_s is sufficiently small. This implies that a window size of the moving average for $\xi_N[n]$ is two seconds. A large amount of data is recorded at every 10 ms for all time period.

The monopulse tracking mode described in Section II works when the tracking angle is within the HPBW of $\pm 0.7°$. The angular estimation filtering mode proposed in Section III always operates in the background and then is triggered in the absence of the monopulse output regardless of the present tracking angle. Note that the GDT prototype enters a box scan mode if the filtering mode lasts for 15 seconds. By running in the box scan mode, the GDT searches the downlink signal power transmitting from the ADT antenna, and initiates the monopulse tracking mode.

---

[3] Unlike the monopulse based tracking at the GDT, the tracking scheme at the ADT is based on the GPS information about the aircraft and the GDT locations. The fixed position of the GDT is known to the ADT in advance, and then the ADT tracking angle is computed by combining the GDT position with the current position and the attitude of the aircraft. Therefore, even though the aircraft moves around, the ADT antenna can point to the GDT at the ground site.
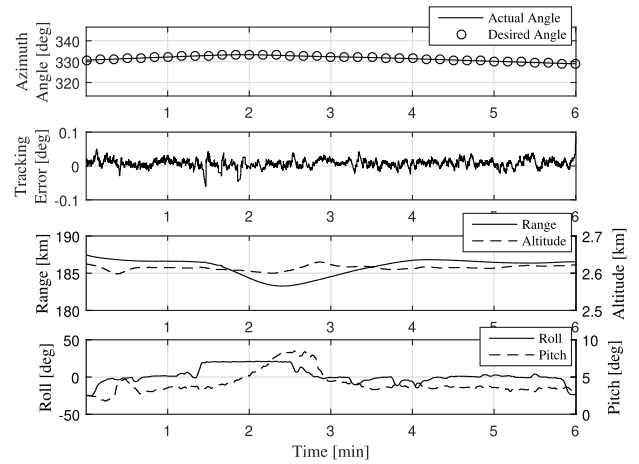
B. TRACKING ACCURACY PERFORMANCE ACCORDING TO A DISTANCE
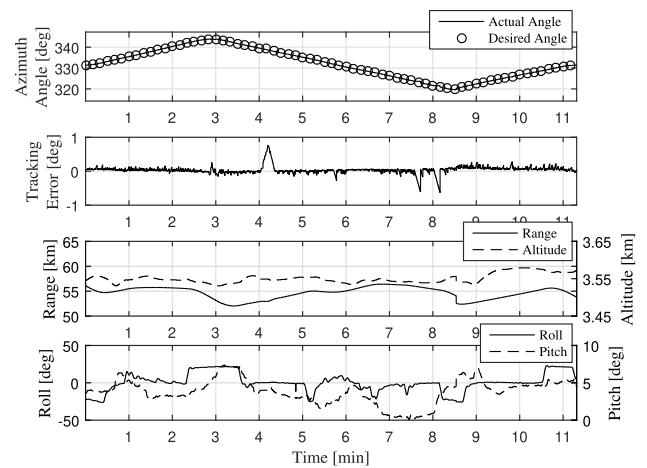
First, we verify that an antenna beam alignment between the moving ADT and the fixed GDT can be maintained accurately at various distances. The trajectories of the aircraft are configured with three regions R1, R2, and R3, which are located 185 km, 105 km, and 55 km away from the GDT, respectively. The aircraft climbs to an altitude of about 2.6 km in the R1 region, 3.5 km in the R2 and R3 regions. Note that the aircraft moves about 20 km at each of the regions.

Under these conditions, Figures 5 and 6 show the desired and actual azimuth tracking angles and the tracking errors with respect to the flight time at the R1 and R3 regions, respectively. It is noted that the GDT prototype gives fairly accurate tracking performance as shown in the azimuth tracking error tendency. To evaluate the tracking accuracy of the proposed design, we calculate the root mean squared error (RMSE) on the tracking errors between the desired azimuth tracking angles and the actual values of the GDT. In this simulation, we obtain the desired angle by calculating
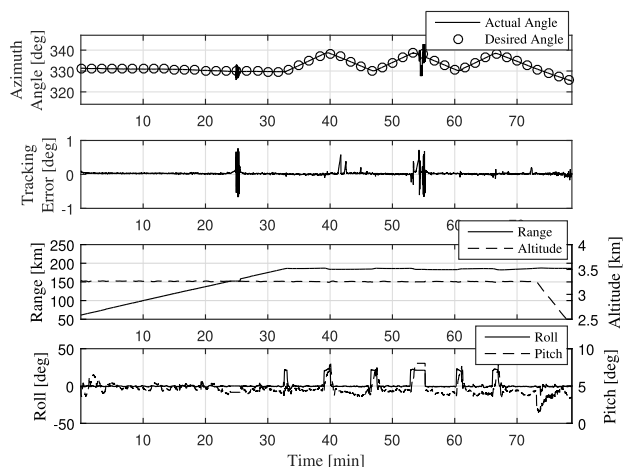
FIGURE 7. Tracking accuracy result in the long-term scenario.

FIGURE 8. Auto-tracking performance result in the test case 5 and 6.

the azimuth angle with the recorded GPS information of the ADT and GDT.

As a result, the RMSE is computed as 0.015° for the region R1 and 0.023° for the region R2. The RMSE of the region R3 is 0.068° except for invalid GPS information intervals[4]. The closer the distance between the ADT and the GDT is, the greater the angular velocity becomes given the same aircraft speed. Thus, the tracking error can be more significant as the range decreases. During the test, these RMSEs are sufficient for the transmission of multiple data stream concurrently, e.g. internet protocol (IP) based video and voice transfer, since the tracking error of 0.1° causes a negligible degradation from Fig. 4. The results in both figures demonstrate that the GDT has reliable tracking performance even though the RMSE increases slightly as the range reduces.

Second, in Fig. 7, we further demonstrate the effectiveness of the proposed system through long-term measurements of about 80 minutes. The flight track includes an straight line path away from the ground site and a clockwise racetrack pattern near the region R1. As expected, the received signal strength shows a steady decrease as the aircraft travels outbound. It is observed that except for the 25 and 55 minute periods operated in the box scan mode after rebooting the prototype twice, the GDT still track well as shown in Fig. 7. Excluding the preceding reboot and scan phases, the RMSE result is given as 0.045° which is a remarkable result for the long-term measurements. Finally, we can observe that the tracking accuracy of our proposed system is sufficient for long range transmission with a narrow beam antenna.

C. AUTO-TRACKING PERFORMANCE IN THE ABSENCE OF THE MONOPULSE OUTPUT

Since a correct antenna alignment is a prerequisite for reconnecting the AG wireless link, the GDT should be able to

---

[4] There is a slight delay and no reception for gathering the GPS information at 4.2, 7.7, and 8.1 minute. Since wrong GPS information yields incorrect desired angle, a tracking error becomes big.
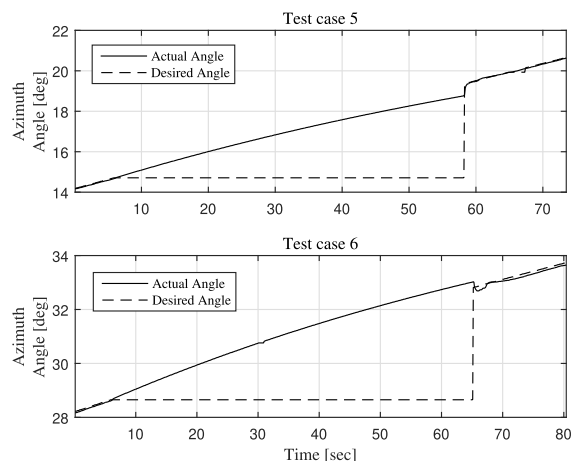
automatically track even though the monopulse output is not available temporarily. To evaluate the auto-tracking performance, we experiment disconnection setups by toggling the ADT's transmit power. Meanwhile, the ADT antenna continues with the GPS based tracking by utilizing the known GDT location and real-time GPS information of the aircraft. For this flight test, the distance between the ADT and the GDT ranges from 48 to 60 km. The aircraft flies in a straight line and the altitude maintains as 1.8 to 3 km.

As a preliminary test, 13 consecutive disconnections are generated for a short period of up to 12 seconds. We confirm that the GDT can offer robust auto-tracking performance under several disconnections. Next, we gradually increase the disconnected time from 18 to 82 seconds for seven test cases. Table 1 summarizes the auto-tracking performance results and the associated measurements. During the disconnected period without the downlink signal, we obtain the desired angle variations and angular velocities, and measure the actual angular velocities. After the recovery of the downlink signal, we observe the actual current angles and the resultant tracking errors. Clearly, the GDT can resume the monopulse tracking procedure and successfully establish the AG link again, if the tracking error is within the HPBW of ±0.7° after the recovery of the downlink signal. In particular, we include the detailed results for the test case 5 and 6 in Fig. 8. Here, the GDT is not able to receive and store the GPS information of the aircraft during disconnections, which is revealed from the staircase pattern in the desired angle graph.

On the other hand, in the test case 7, the reconnection for the monopulse tracking mode is not achieved due to rapid decelerations over long disconnected period of 82 seconds. In conclusion, the performance results show that the proposed angular estimation filter can adequately compensate for the absence of the downlink signal for at least 60 seconds, which provide a significant capability in various applications of the AG communication system.

TABLE 1. Auto-tracking performance results according to the increased disconnection time.

Test case	Disconnected duration [sec]	Desired angle variation [deg]	Desired angular velocity [deg/sec]	Actual angular velocity [deg/sec]	Actual angle after the signal recovery [deg]	Tracking error after the signal recovery [deg]	Re-connection result
1	18	1.7	0.094	0.078	350.1	−0.3	Success
2	22	2.0	0.091	0.080	355.5	−0.4	Success
3	32	3.0	0.094	0.078	362.4	−0.5	Success
4	39	3.6	0.092	0.077	7.7	−0.6	Success
5	52	4.7	0.090	0.081	18.8	−0.5	Success
6	60	4.2	0.070	0.073	33.0	0.2	Success
7	82	4.6	0.056	0.038	37.1	−1.5	Fail

V. CONCLUSION

In this paper, we have designed the monopulse tracking system for the long rage AG communication, and implemented a prototype with the single channel architecture and the angular estimation filter. Then we have tested the prototype performance via realistic flight tests up to the distance of 185 kilometers. The experimental measurement has demonstrated that the proposed system achieves the reliable tracking performance. From extensive field test results, we have verified that the proposed approach can be adopted in actual airborne platforms as well as UAVs that need the long range AG communication. In the future, the space-air-ground integrated network [34] is expected to become aerial networks which relay the increasing traffic demands of various services among space, air and ground. Extensions to an air-to-space link or an air-to-air link with multiple UAVs are worth pursuing [35], [36]. Also, electrically steering antennas based AG communication systems could be an important research direction.

ACKNOWLEDGMENT

REFERENCES

[1] S. Hayat, E. Yanmaz, and R. Muzaffar, "Survey on unmanned aerial vehicle networks for civil applications: A communications viewpoint," *IEEE Commun. Surveys Tuts.*, vol. 18, no. 4, pp. 2624–2661, 4th Quart., 2016.

[2] X. Cao, P. Yang, M. Alzenad, X. Xi, D. Wu, and H. Yanikomeroglu, "Airborne communication networks: A survey," *IEEE J. Sel. Areas Commun.*, vol. 36, no. 9, pp. 1907–1926, Sep. 2018.

[3] Y. Zeng, R. Zhang, and T. J. Lim, "Wireless communications with unmanned aerial vehicles: Opportunities and challenges," *IEEE Commun. Mag.*, vol. 54, no. 5, pp. 36–42, May 2016.

[4] Y. Zeng, Q. Wu, and R. Zhang, "Accessing from the sky: A tutorial on UAV communications for 5G and beyond," *Proc. IEEE*, vol. 107, no. 12, pp. 2327–2375, Dec. 2019.

[5] B. Li, Z. Fei, and Y. Zhang, "UAV communications for 5G and beyond: Recent advances and future trends," *IEEE Internet Things J.*, vol. 6, no. 2, pp. 2241–2263, Apr. 2019.

[6] X. Li, Q. Wang, Y. Liu, T. A. Tsiftsis, Z. Ding, and A. Nallanathan, "UAV-aided multi-way NOMA networks with residual hardware impairments," *IEEE Wireless Commun. Lett.*, early access, May 22, 2020, doi: 10.1109/LWC.2020.2996782.

[7] X. Li, Q. Wang, H. Peng, H. Zhang, D.-T. Do, K. M. Rabie, R. Kharel, and C. C. Cavalcante, "A unified framework for HS-UAV NOMA networks: Performance analysis and location optimization," *IEEE Access*, vol. 8, pp. 13329–13340, 2020.

[8] J. Park, H. Lee, S. Eom, and I. Lee, "UAV-aided wireless powered communication networks: Trajectory optimization and resource allocation for minimum throughput maximization," *IEEE Access*, vol. 7, pp. 134978–134991, 2019.

[9] S. Eom, H. Lee, J. Park, and I. Lee, "UAV-aided wireless communication designs with propulsion energy limitations," *IEEE Trans. Veh. Technol.*, vol. 69, no. 1, pp. 651–662, Jan. 2020.

[10] S. Eom, H. Lee, J. Park, and I. Lee, "UAV-aided two-way mobile relaying systems," *IEEE Commun. Lett.*, vol. 24, no. 2, pp. 438–442, Feb. 2020.

[11] A. Islam and S. Y. Shin, "BUAV: A blockchain based secure UAV-assisted data acquisition scheme in Internet of Things," *J. Commun. Netw.*, vol. 21, no. 5, pp. 491–502, Oct. 2019.

[12] A. Fotouhi, H. Qiang, M. Ding, M. Hassan, L. G. Giordano, A. Garcia-Rodriguez, and J. Yuan, "Survey on UAV cellular communications: Practical aspects, standardization advancements, regulation, and security challenges," *IEEE Commun. Surveys Tuts.*, vol. 21, no. 4, pp. 3417–3442, 4th Quart., 2019.

[13] J. Roth, R. Gleich, J. Ortiz, M. Schon, and B. Klenke, "Unmanned aircraft system (UAS) exercise to assess common data link (CDL) technology," MITRE, Bedford, MA, USA, Tech. Rep. MTR090082, Feb. 2009.

[14] J. Kim, J. Ryu, Y.-J. Ryu, and D.-C. Han, "Layer 2 framing and equivalent error rate over airborne common data link systems," in *Proc. Int. Conf. Inf. Commun. Technol. Converg. (ICTC)*, Oct. 2015, pp. 778–779.

[15] J. Pokorny, A. Ometov, P. Pascual, C. Baquero, P. Masek, A. Pyattaev, A. Garcia, C. Castillo, S. Andreev, J. Hosek, and Y. Koucheryavy, "Concept design and performance evaluation of UAV-based backhaul link with antenna steering," *J. Commun. Netw.*, vol. 20, no. 5, pp. 473–483, Oct. 2018.

[16] J. Yan, H. Zhao, X. Luo, C. Chen, and X. Guan, "RSSI-based heading control for robust long-range aerial communication in UAV networks," *IEEE Internet Things J.*, vol. 6, no. 2, pp. 1675–1689, Apr. 2019.

[17] J. Chen, J. Xie, Y. Gu, S. Li, S. Fu, Y. Wan, and K. Lu, "Long-range and broadband aerial communication using directional antennas (ACDA): Design and implementation," *IEEE Trans. Veh. Technol.*, vol. 66, no. 12, pp. 10793–10805, Dec. 2017.

[18] S. Li, C. He, M. Liu, Y. Wan, Y. Gu, J. Xie, S. Fu, and K. Lu, "Design and implementation of aerial communication using directional antennas: Learning control in unknown communication environments," *IET Control Theory Appl.*, vol. 13, no. 17, pp. 2906–2916, Nov. 2019.

[19] M. Liu, Y. Wan, S. Li, F. L. Lewis, and S. Fu, "Learning and uncertainty-exploited directional antenna control for robust long-distance and broadband aerial communication," *IEEE Trans. Veh. Technol.*, vol. 69, no. 1, pp. 593–606, Jan. 2020.

[20] S. M. Sherman and D. K. Barton, *Monopulse Principles and Techniques*, 2nd ed. Boston, MA, USA: Artech House, 2011.

[21] J. Kim, J. Jung, and D. Han, "Robust tracking for transient disconnections of UAV data link," in *Proc. APISAT*, Oct. 2017, pp. 1–6.

[22] X. Pan, C. Yan, and J. Zhang, "Nonlinearity-based single-channel monopulse tracking method for OFDM-aided UAV A2G communications," *IEEE Access*, vol. 7, pp. 148485–148494, 2019.

[23] D. F. Crouse, "A General Solution to Optimal Fixed-Gain ($\alpha - \beta - \gamma$ etc.) filters," *IEEE Signal Process. Lett.*, vol. 22, no. 7, pp. 901–904, Jul. 2015.

[24] H. Kumar and G. Kumar, "Monopulse comparators [Applicaton Notes]," *IEEE Microw. Mag.*, vol. 20, no. 3, pp. 13–100, Mar. 2019.

[25] J. Kim, J. Jung, J.-M. Lee, and U.-Y. Pak, "A mathematical perspective of single-channel pseudo-monopulse tracking receiver design," in *Proc. Int. Conf. Inf. Commun. Technol. Converg. (ICTC)*, Oct. 2014, pp. 874–875.

[26] U. Nickel, "Overview of generalized monopulse estimation," *IEEE Aerosp. Electron. Syst. Mag.*, vol. 21, no. 6, pp. 27–56, Jun. 2006.

[27] B. R. Mahafza, *Radar Systems Analysis and Design Using MATLAB*, 3rd ed. Boca Raton, FL, USA: CRC, Press, 2013.

[28] E. Brookner, *Tracking and Kalman Filtering Made Easy*, 1st ed. Hoboken, NJ, USA: Wiley, 1998.

[29] D. Simon, "Kalman Filtering," *Embedded Syst. Program.*, vol. 14, no. 6, pp. 72–79, Jun. 2001.

[30] C. An, J. Yang, R. Ran, U. Y. Pak, Y. Ryu, and D. K. Kim, "Enhanced monopulse MIMO radar using reliable $\alpha\beta$ filtering," in *Proc. IEEE Mil. Commun. Conf. (MILCOM)*, Oct. 2012, pp. 1–6.

[31] K. Huarng and T. Hui-Kuang Yu, "Ratio-based lengths of intervals to improve fuzzy time series forecasting," *IEEE Trans. Syst., Man Cybern., B (Cybern.)*, vol. 36, no. 2, pp. 328–340, Apr. 2006.

[32] H. J. Kil, Y. J. Lee, J. S. Kim, and E. S. Lee, "Enhancement for performance of monopulse and target tracking for communication signal tracking," *J. Inst. Electron. Inf. Eng.*, vol. 51, no. 5, pp. 35–43, May 2014.

[33] B. P. Kumar, C. Kumar, V. S. Kumar, and V. V. Srinivasan, "Performance of an axially displaced ellipse reflector antenna with compact monopulse tracking feed for a small aperture transportable terminal," *IEEE Trans. Antennas Propag.*, vol. 68, no. 3, pp. 2008–2015, Mar. 2020.

[34] J. Liu, Y. Shi, Z. M. Fadlullah, and N. Kato, "Space-Air-Ground integrated network: A survey," *IEEE Commun. Surveys Tuts.*, vol. 20, no. 4, pp. 2714–2741, 4th Quart., 2018.

[35] J. Lee, J. Lim, and E. Kim, "Comparison between multimode-monopulse and step-tracking techniques for a UAV satellite terminal," in *Proc. Wireless Telecommun. Symp. (WTS)*, Apr. 2016, pp. 1–5.

[36] J. Zhao, F. Gao, Q. Wu, S. Jin, Y. Wu, and W. Jia, "Beam tracking for UAV mounted SatCom on-the-Move with massive antenna array," *IEEE J. Sel. Areas Commun.*, vol. 36, no. 2, pp. 363–375, Feb. 2018.

JAEMOON LEE received the B.S. and M.S. degrees in electrical engineering from Hanyang University, Seoul, South Korea, in 2000 and 2002, respectively, and the Ph.D. degree in computer engineering from Ajou University, Gyeonggi, South Korea, in 2016. Since 2002, he has been with the Agency for Defense Development, Daejeon, South Korea, where he is currently a Principle Researcher and a Team Leader. His research interests include airborne communication technologies and satellite systems for network centric operation environments.

INKYU LEE (Fellow, IEEE) received the B.S. degree (Hons.) in control and instrumentation engineering from Seoul National University, Seoul, South Korea, in 1990, and the M.S. and Ph.D. degrees in electrical engineering from Stanford University, Stanford, CA, USA, in 1992 and 1995, respectively. From 1995 to 2001, he was a Member of the Technical Staff with Bell Laboratories, Lucent Technologies, where he studied high-speed wireless system designs. From 2001 to 2002, he was a Distinguished Member of the Technical Staff with Agere Systems (formerly the Microelectronics Group, Lucent Technologies), Murray Hill, NJ, USA. Since 2002, he has been with Korea University, Seoul, where he is currently a Department Head of the School of Electrical Engineering. In 2009, he was a Visiting Professor with the University of Southern California, Los Angeles, CA, USA. He has authored or coauthored more than 180 journal articles in IEEE publications and has 30 U.S. patents granted or pending. His research interests include digital communications, signal processing, and coding techniques applied for next-generation wireless systems. He has been elected as a member of National Academy of Engineering in Korea in 2015. He is an IEEE Distinguished Lecturer. He was a recipient of the IT Young Engineer Award at the IEEE/IEEK Joint Award in 2006 and of the Best Paper Award at the Asia-Pacific Conference on Communications in 2006, the IEEE Vehicular Technology Conference in 2009, and the IEEE International Symposium on Intelligent Signal Processing and Communication Systems in 2013. He was also a recipient of the Best Research Award from the Korean Institute of Communications and Information Sciences (KICS) in 2011, the Best Young Engineer Award from the National Academy of Engineering in Korea in 2013, and the Korea Engineering Award from the National Research Foundation of Korea in 2017. He has served as an Associate Editor for the IEEE Transactions on Communications from 2001 to 2011 and the IEEE Transactions on Wireless Communications from 2007 to 2011. In addition, he was a Chief Guest Editor of the IEEE Journal on Selected Areas in Communications (Special Issue on 4G Wireless Systems) in 2006. He also serves as a Co-Editor-in-Chief for the *Journal of Communications and Networks*.

JAESIN KIM received the B.S. and M.S. degrees in electrical engineering from Korea University, Seoul, South Korea, in 2008 and 2010, respectively, where he is currently pursuing the Ph.D. degree. Since 2010, he has been with the Agency for Defense Development, Daejeon, South Korea, as a Senior Researcher. His research interests include signal processing and optimization technologies for the next-generation airborne wireless networks. He received the Best Paper Award at the 18th Asia-Pacific Conference on Communications in 2012.

• • •